Available online at www.sciencedirect.com
SCIENCE DIRECT
Sensors and Actuators B 114 (2006) 9–18
SENSORS AND ACTUATORS B CHEMICAL
www.elsevier.com/locate/snb

A microstructured silicon membrane with entrapped hydrogels for environmentally sensitive fluid gating

Antonio Baldi [a,*], Ming Lei [a], Yuandong Gu [b,1], Ronald A. Siegel [b,c], Babak Ziaie [a,c,2]

[a] *Department of Electrical and Computer Engineering, University of Minnesota, Minneapolis, MN 55455, USA*
[b] *Department of Pharmaceutics, University of Minnesota, Minneapolis, MN 55455, USA*
[c] *Department of Biomedical Engineering, University of Minnesota, Minneapolis, MN 55455, USA*

Received 1 October 2004; received in revised form 22 March 2005; accepted 4 April 2005
Available online 6 June 2005

Abstract

In this paper, we report on the fabrication and characterization of a new hydrogel-based microvalve. The basic structure is a silicon membrane having an array of orifices with an internal structure designed to anchor the hydrogel while allowing it to gate the flow across the membrane. Each orifice (140 μm diameter) has a central post suspended by four tethers on each side of the membrane. A stimuli-sensitive hydrogel is polymerized inside each orifice. In the swollen state, the hydrogel completely occupies the void space of the orifice, completely blocking pressure-driven fluid flow. In the shrunken state, the hydrogel contracts around the post, allowing fluid to flow through an opened annular gap. Fabrication of the microstructured silicon membrane requires only two masking steps and involves a combination of deep trench and KOH etch. Two different hydrogels, based on *N*-isopropylacrylamide (temperature-sensitive) and phenylboronic acid (pH and glucose-sensitive) were trapped and tested in this microvalve. The measured response times were 10 s (temperature), 4 min (pH), and 10 min (glucose). The maximum pressure drop the microvalve can sustain before breakage of the hydrogel is 21 kPa and 16 kPa for temperature-sensitive and (pH/glucose)-sensitive hydrogels, respectively.

Keywords: Hydrogel; Microvalve; Stimuli-sensitive; Microfluidics

1. Introduction

Environmentally sensitive hydrogels integrated with micromechanical/microfluidic structures for active flow control at micro-scale have recently attracted considerable attention. These polymer networks respond with significant volume change to stimuli such as temperature, pH, glucose, electric field, and light among others [1,2]. Hydrogel response time depends on water absorption–expulsion kinetics and becomes reasonably short when dimensions are in the microscale. Incorporation of hydrogels into microfluidic structures may, therefore, lead to rapid gating and control of fluid motion, with potential applications in implantable drug delivery systems, micro-reaction devices, and lab-on-a-chip micro-total analysis systems (μTAS) [3–12].

Several microvalve structures that utilize the chemomechanical properties of hydrogels have been reported. These include: (1) microvalves formed inside microchannels by selective photopolymerization of hydrogel around posts [4], (2) mimics of venous flaps valves [5], (3) electronically controlled valves actuated by an integrated heating element formed underneath a temperature-sensitive hydrogel [6], and (4) valves based on a temperature-sensitive hydrogel loaded in a chamber adjacent to a flow channel but separated from the channel by a flexible PDMS membrane [7].

* Corresponding author at: Centro Nacional de Microelectronica (CNM-IMB, CSIC), Campus UAB, E-08193 Barcelona, Spain.
Tel.: +34 93 5947700; fax: +34 93 5801496.
E-mail address: antoni.baldi@cnm.es (A. Baldi).
[1] Present address: Honeywell Inc., Brooklyn Park, MN, USA.
[2] Present address: School of Electrical and Computer Engineering, Purdue University, West Lafayette, IN, USA.

0925-4005/$ – see front matter © 2005 Elsevier B.V. All rights reserved.
doi:10.1016/j.snb.2005.04.020

Recently, a microvalve that is responsive to its external liquid environment was demonstrated [8]. This microvalve consists of a thin hydrogel, sandwiched between a rigid porous membrane and a flexible silicone rubber diaphragm. The diaphragm is attached to an embossment that opens and shuts the inlet to a flow channel. Volume changes of the hydrogel, which result from exchange of chemical species between the hydrogel and the liquid environment through the rigid membrane, are accompanied by deflection of the diaphragm/embossment and hence closure and opening of the channel. Such a valve can gate the flow and delivery of drug solutions in response to physiological changes. Glucose-controlled insulin delivery is a target application of this microvalve.

The microvalves described above gate the flow of fluid through channels that run primarily in-plane with the chip surface. One might also consider valves that gate flow perpendicular to the chip plane. Such valves would act analogously to membranes containing stimuli-sensitive polymers that modulate the flow of fluid when their pore structure is altered in response to an appropriate environmental stimulus [9]. Our group recently demonstrated an implementation of a hydrogel-gated membrane-type microvalve [10]. This device achieves flow control by interlocking the hydrogel with a glass frame fabricated by cutting parallel sets of trenches on either side of a glass wafer. The trenches on the front side are cut orthogonally to those on the back-side, and all trenches are diced to a depth exceeding the half-thickness of the wafer. An array of holes spanning the wafer thickness is, therefore, created at the intersections of the opposing cuts. The pregel solution is loaded and polymerized in the trenches. When the gel is swollen, it fills the trenches and blocks fluid flow perpendicular to the wafer. When the hydrogel shrinks, fluid flows through gaps that open up at the wafer-spanning intersections. The dimensions of the hydrogel in this case are constrained by the wafer thickness and dicing saw's minimum cut depth and width. The response times of the criss-cross-cut structure, created from a 500 μm thick glass wafer cut with 120 μm wide and 300 μm deep trenches and loaded with temperature- and glucose-sensitive hydrogels, were 50 s and 4 h, respectively.

In this paper, we describe a micromachined silicon membrane valve that contains an array of micro-orifices whose internal structure is designed to confine the hydrogel while allowing it to control flow perpendicular to the chip surface. This structure is expected to provide fast, reproducible response to external stimuli.

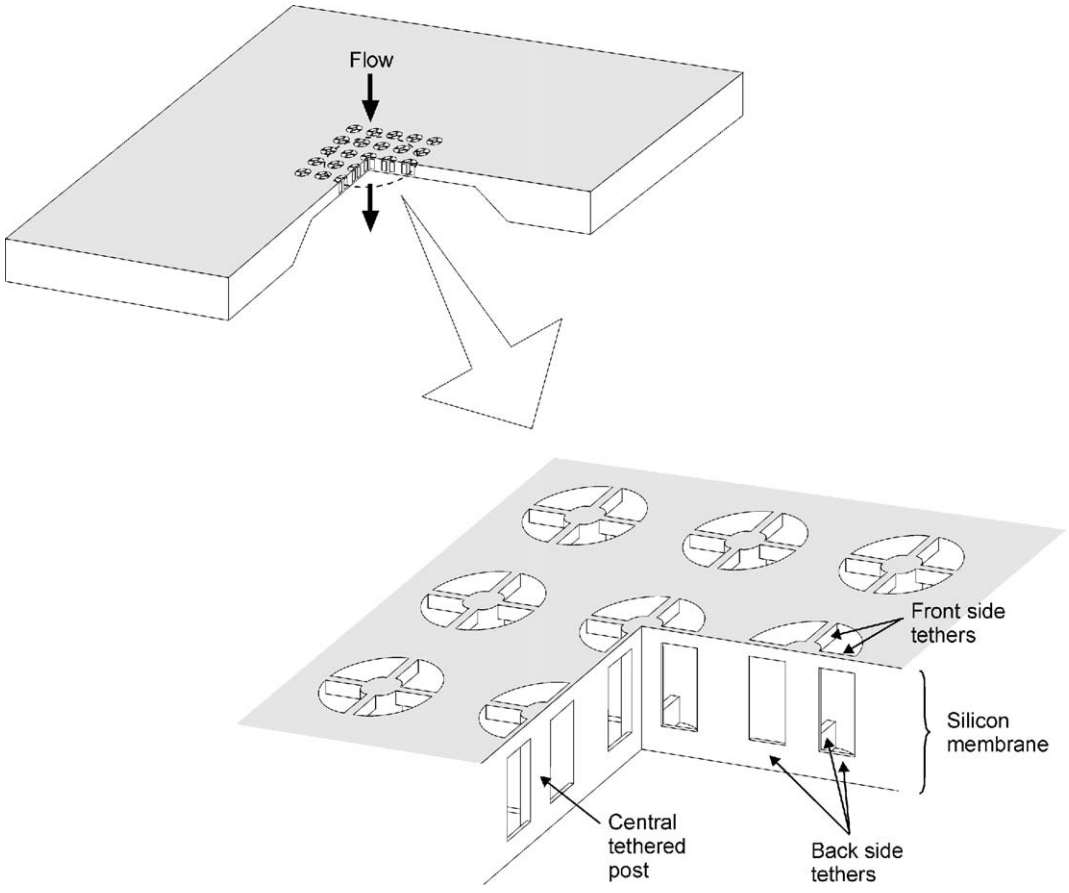

Fig. 1. Three-dimensional schematic representation of a sectional view of the silicon membrane with structured orifices.

2. Device concept and design

Fig. 1 shows a schematic representation of the microstructured silicon membrane, which features an array of cylindrical orifices containing central posts, suspended by narrow tethers on each side of the membrane. The orifices are loaded with a stimuli-responsive hydrogel. The resulting structure is hereafter called the "microvalve". In the swollen state, the hydrogel occupies the whole volume of the orifice, and fluid flow is essentially blocked. In the shrunken state, the gel contracts around the central post, allowing fluid to flow through an annular gap opened up between the hydrogel and the orifice wall. The tethers secure the post and anchor the hydrogel so that it is not dislodged by flow.

Both physical and chemical stimuli-sensitive hydrogels can be polymerized inside the orifices. In this paper, we present results with temperature- and pH/glucose-sensitive hydrogels [11]. The small dimensions of the hydrogel-confining structure enable shorter response times compared to previously reported membrane-type structures [10,12]. The microvalve can be designed to provide a wide range of flow rates at the open state by adjusting the membrane thickness and the diameter and number of orifices.

In the present design, the membrane is 100 μm thick, has area 2 mm × 2 mm, and contains an array of 25 identical orifices that open and shut together when exposed to a common stimulus. Diameters of the orifices and their central post are 140 μm and 40 μm, respectively. Four tethers in each orifice, having length, 50 μm; width, 10 μm; and thickness, 20 μm, unite the central post with the orifice perimeter on both sides of the membrane.

3. Methods

3.1. Valve microfabrication

Fabrication of the double-tethered structure was accomplished in two masking steps by combining different kinds of silicon etch, as shown in Fig. 2. Initially, a 100 μm thick silicon membrane was formed by KOH-etching the back side of a 500 μm thick ⟨1 0 0⟩ silicon wafer. A patterned 2 μm thick nitride layer deposited by LPCVD on the wafer was used as a mask for this etch step.

Formation of the top set of tethers was based on a modified SCREAM fabrication process [13]. Nitride was patterned on the front side (top) of the membrane with the spoked feature shown in Fig. 2c. The exposed silicon, which consisted of four annular sectors, was then etched to a depth of 20 μm in a deep trench etcher (ICP Plasma-Therm SLR series with

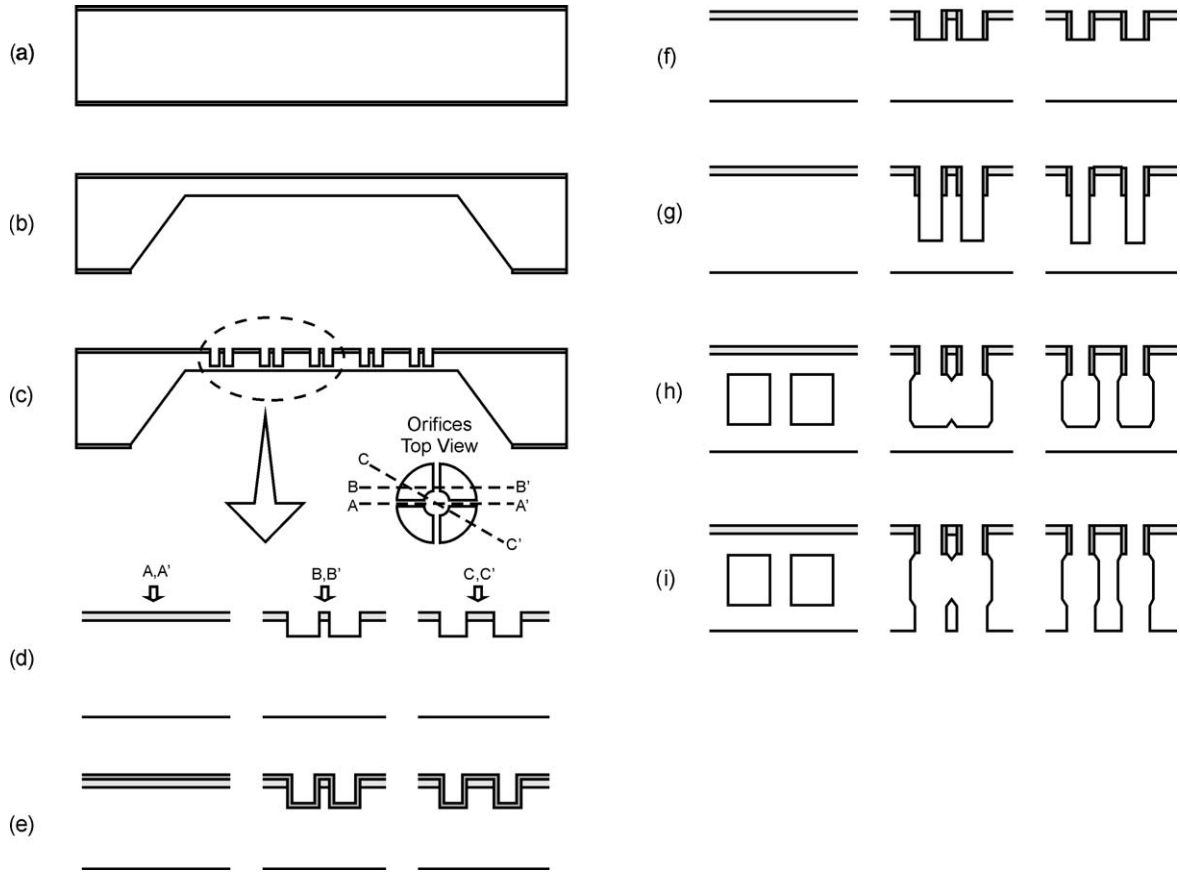

Fig. 2. Fabrication process: (a) nitride deposition, (b) backside nitride patterning and KOH etch, (c and d) front side nitride patterning and first DRIE, (e) PECVD oxide deposition, (f) floor oxide etch, (g) second DRIE, (h) short KOH etch or silicon plasma etch, (i) third DRIE.

Bosch process). During this step, the outer circle of the pattern defined the outer orifice wall, the central circle defined a thick post, and the four radial spokes defined thin silicon slats. Next, a 0.5 μm thick oxide layer was deposited in the etched sectors by PECVD. The oxide layer deposited on the floor of the features was then removed by anisotropic oxide etch. Oxide on the walls was essentially undisturbed during this step.

The process continued with a second 60 μm deep silicon trench etch. At this point, the top 20 μm of the post and the thin silicon slats were protected by the oxide layer, whereas the lower 60 μm were bare silicon. The lower parts of the walls were removed either by wet (KOH) anisotropic or dry (plasma) isotropic etch, leaving behind four freestanding silicon tethers bridging the central post to the orifice outer wall. The last step consisted of a third deep trench etch that punched through the back of the silicon membrane. Because of shadowing by the front tethers, a complementary pair of rear tethers remained connecting the back side of the central post to the outer wall of the orifice.

3.2. Synthesis and incorporation of hydrogels in orifices

The temperature-sensitive hydrogel was prepared from a pregel solution consisting of 100 mg isopropylacrylamide (NIPA, purified in the lab, Polysciences), 1 mg *N*,*N*′-methylenebisacrylamide (Bis, >99%, Polysciences, cross-linker), 5 μl tetraethyl methylenediamine (TEMED, 99%, Sigma-Aldrich, accelerator), and 1 mg ammonium persulfate (APS, electro pure, Polysciences, initiator), all dissolved in 1 ml of deionized water. The pH/glucose-sensitive hydrogel was prepared from a pregel solution containing 80 mg acrylamide (AAm, 99%, Sigma-Aldrich), 52 mg methylacrylamidophenylboronic acid (MPBA, synthesized according to [14]), 0.5 mg Bis, 5 μl TEMED, and 0.5 mg APS, 0.25 ml 1N NaOH solution and deionized water with total volume 0.7 ml.

Devices were immersed in the pregel solution. Bubble entrapment inside the orifices was avoided by first wetting one side of the device and forcing some of the solution through the membrane. Polymerization occurred after 10 min at room temperature, but was carried to completion overnight. After polymerization, excess hydrogel was removed by separate methods for the two different hydrogels. The device loaded with the temperature-sensitive hydrogel was immersed in deionized water to fully swell the hydrogel. Excess hydrogel was easily peeled off from both sides of the membrane. Excess pH/glucose-sensitive hydrogel was removed immediately after polymerization using a flat-end wood stick. Both hydrogels were polymerized in their swollen states, so that space would open up for fluid flow when the hydrogels shrank.

3.3. Flow tests

To test microvalve's flow gating capability in response to an environmental change, the membrane was clamped in a fixture with fluidic connectors. Fig. 3a and b show the experimental setups used for the temperature- and pH/glucose-sensitive microvalves, respectively. The temperature-sensitive device was connected to rubber tubing (i.d. = 3 mm and o.d. = 4.8 mm) on both sides (Fig. 3a). The upstream tubing led to a water reservoir at constant pressure head, while the downstream tubing served as a drain. This assembly was immersed in a water bath at specified temperature, or was alternated between baths at low and high temperatures. The upstream tubing was coiled to ensure adequate thermal equilibration between the luminal water and the bath. For the pH/glucose-sensitive membrane, it was necessary to directly expose the hydrogel to the solution being transported, as shown in Fig. 3b. A negative pressure was applied at the outlet tubing to drive fluid flow. For both test setups, flow rate was determined from the velocity of an air bubble injected in a glass tube connected to the outlet [8].

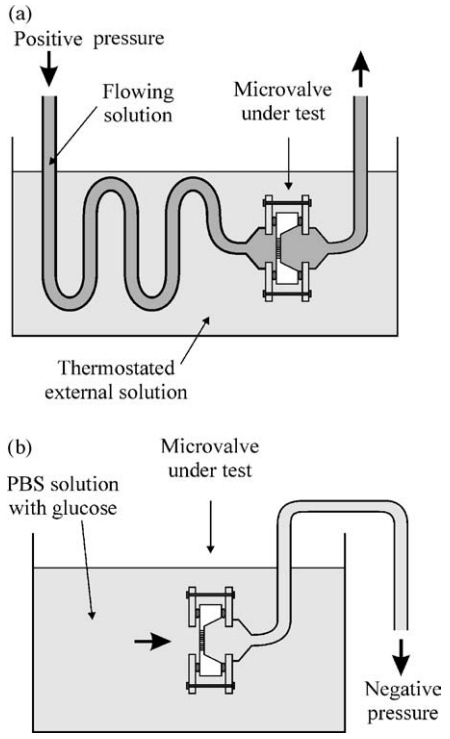

Fig. 3. Experimental setups for the measurement of the microvalve response to (a) temperature and (b) pH/glucose concentration. The device is clamped between two plates with fluidic connectors to tubing.

4. Results

4.1. Microvalve structure

Microvalves were successfully fabricated using both wet and dry etching techniques to release the top tethers. Fig. 4a and b show SEM micrographs revealing the orifice walls,

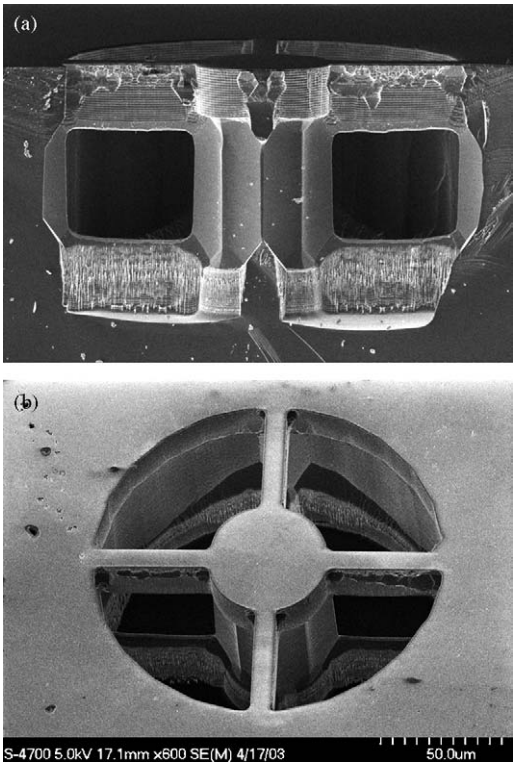

Fig. 4. SEM micrographs of (a) the side view of a fractured structure fabricated without initial back side KOH etch, and (b) top view of a complete microstructured orifice.

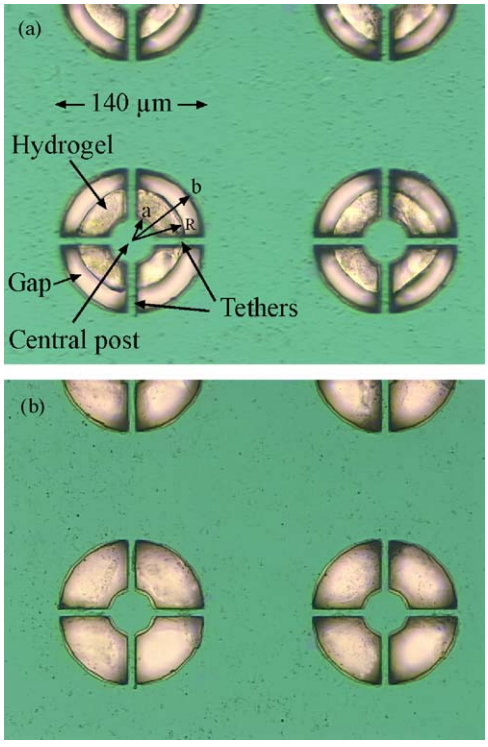

Fig. 5. Micrographs of an orifice loaded with hydrogel and immersed in water at (a) 50 °C (hydrogel shrunken), (b) 25 °C (hydrogel swollen). *a*, *b*, and *R* are defined in the Appendix A.

the central post, and the tethers. In Fig. 4a, the orifices were fabricated on a full-thickness wafer (no initial KOH etch) in order to obtain a clean section of the structure when cleaving the wafers for SEM inspection. In this case, release of the top tethers was carried out using KOH. The presence of fast and slow etch planes in the silicon led to polygonal shapes of the central post and orifice wall below the top tethers, and a V-shaped underside of those tethers. The bottom set of tethers was formed during the last deep RIE step, with the top tethers serving as a "shadow mask" for anisotropic etch of the passivation layer during the three step cycles of the Bosch process. The bottom tethers were slightly wider than the top tethers. Fig. 4b shows the top view of a complete orifice on a 100 μm thick silicon membrane. Again, KOH etch was used to release the top tethers. The orifice is open on both sides of the membrane and has the desired double-tethered structure for entrapment of the hydrogel.

Optical micrographs of an orifice loaded with temperature-sensitive NIPA hydrogel in the shrunken and swollen states are shown in Fig. 5a and b, respectively. In the swollen state (low temperature, 25 °C), the hydrogel occupies the entire orifice. In the shrunken state (high temperature, 50 °C), the hydrogel is collapsed around the central post, and an annular gap is opened between the hydrogel and the outer orifice wall. It is through this gap that fluid flows.

4.2. Temperature-sensitive microvalve test

For the temperature-sensitive microvalve (NIPA hydrogel), the flowing liquid was deionized water with a 74 cm pressure head. The microvalve was alternately immersed in two beakers with water at 25 °C and 50 °C. Fig. 6 shows the flow response resulting from this alternation. Flow was completely stopped at 25 °C, whereas at 50 °C the flow rate was about 1 ml/min. The response time was about 10 s for opening and 20 s for closing. In a second experiment, bath temperature was increased progressively from 25 °C to 50 °C and flow rate was recorded at several temperatures, as shown in Fig. 7. The sharp change in flow-rate observed at 34 °C is expected based on the volume phase transition temperature of the poly(NIPA) hydrogel [15].

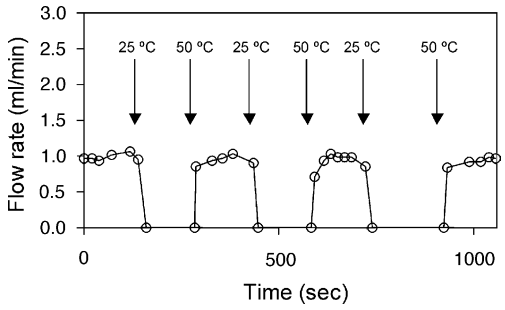

Fig. 6. Flow rate vs. time for thermosensitive microvalve, with temperature alternated between 25 °C and 50 °C and pressure head of 74 mmH_2O.

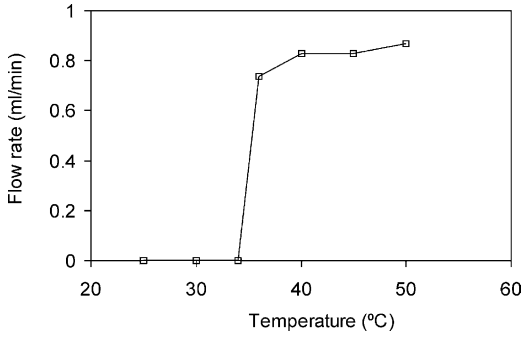

Fig. 7. Flow rate vs. temperature curve for the thermosensitive microvalve, with pressure head 74 mmH_2O.

Flow behavior at higher pressure heads was also investigated at 50 °C. As shown in Fig. 8, the steady state flow rate of water increased almost linearly at low applied pressure (below 5 kPa), but the slope of the flow–pressure characteristic decreased at higher pressure values. This decrease is probably due to elastic deformation of the hydrogel. When exposed to a high pressure gradient, the length of the hydrogel decreases, with corresponding increase in its cross-sectional area and constriction of the annular gap between the hydrogel and the outer wall of the orifice (constriction effect). This in turn increases the flow resistance at high pressures hence decreasing the flow–pressure slope (see Appendix A for a simple model). In the closed state (25 °C), the microvalve could tolerate a 21 kPa of pressure drop before hydrogel rupture and initiation of leakage.

4.3. pH/glucose-sensitive microvalve test

Fig. 9 shows the flow response to pH change for the microvalve loaded with the pH/glucose-sensitive, MPBA/AAm hydrogel. The device was alternately immersed in phosphate buffered saline (PBS) solutions at pH 3.0 and 10.0 while a negative pressure of 55 cmH_2O was applied at the outlet. The pH response time of this microvalve was an order of magnitude slower (4 min) than that of the thermally responsive system.

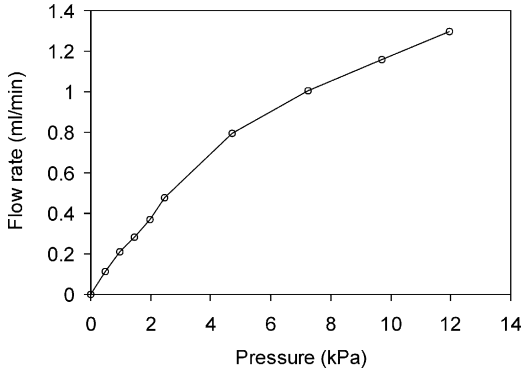

Fig. 8. Flow rate vs. external pressure for a thermosensitive microvalve at 50 °C.

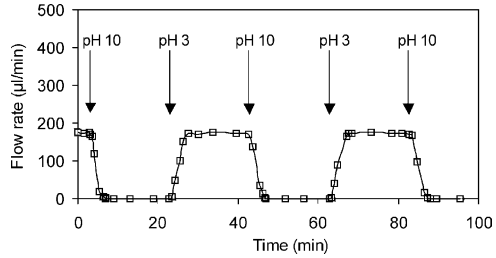

Fig. 9. Flow rate vs. time for pH-sensitive microvalve when alternating pH between 3.0 and 10.0. Pressure head, 90 cmH_2O.

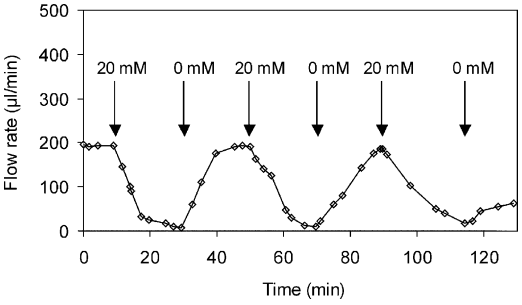

Fig. 10. Flow rate vs. time when alternating glucose concentration between 0 mM and 20 mM. Pressure head, 90 cmH_2O.

Fig. 10 illustrates the response of the same microvalve immersed between two PBS solutions at pH 7.4 with glucose concentration alternated between 0 mM and 20 mM while a negative pressure of 90 cmH_2O (8.8 kPa) was applied at the outlet. Since glucose diffusivity in the gel is slower than that of hydrogen ions and phosphate buffer, an even longer response time (10 min) was observed. With the valve in the closed state (pH 10.0), it was found that the MPBA/AAm hydrogel could withstand a 16 kPa pressure drop before leakage ensued.

5. Discussion

Environmentally controlled gating of diffusive and convective transport through membranes has been studied for over two decades. Most of the literature deals either with stimuli-responsive hydrogels cast in the form of membranes [16–18], or stimuli-responsive polymer chains that are grafted to the walls of microporous membranes [9,19]. Recently, at least two groups have produced membrane composites consisting of water-swollen stimuli-sensitive nanogels dispersed above the percolation threshold within a hydrophobic membrane that acts as a continuous support [20,21]. When swollen, the nanoparticles block transport through the membrane. When collapsed, voids are created in the membrane through which diffusion or convection is now permitted. The present micromachined system is analogous to the latter composite systems, but the geometric configurations of the pores and hydrogel are better defined

and much stronger modulation of transport is achieved. The present system is also an improvement over the previously reported cross-cut system [10], as the much smaller micromachined features permit faster response. A final advantage of the microfabricated system is the potential to integrate controlling elements such as electrically controlled microheaters directly into the device, rather than relying exclusively on the fluid environment in which the device is immersed.

The microvalve orifices were formed by first defining the orifice, central post, and slats, then undercutting the slats to release the top tethers, and finally punching through the back side by shadowed plasma etch to release the bottom tethers. In the second step, either wet chemical or dry isotropic plasma etch could be performed. The main difference in these two methods is that whereas chemical etching left behind polygonal walls, dry etch resulted in rounded features.

Hydrogels were incorporated into the orifices by immersing the membranes into an excess of pregel solution, polymerization, and removal of excess hydrogel from the membrane surfaces. After removal of this excess hydrogel, which exerts a negative osmotic pressure, and exposure to water, the remaining hydrogel will develop an excess positive swelling pressure inside the orifice, tightening the seal. This excess swelling pressure must be reduced below zero before the gel can shrink within the orifice, and this may contribute to the delay in the valve's opening. One future design consideration may be to alter synthesis conditions to control this excess swelling pressure. It should also be noted that the excess swelling pressure may be reduced if the fluid to be gated contains macromolecules that are unable to enter the gel network, and therefore, reduce the difference in osmotic pressure between the fluid and the hydrogel [22].

In the present paper, we have only considered a gating function of the hydrogel in the orifice, so we have termed the composites "microvalves." For the thermally responsive systems with NIPA gels, the response to temperature exhibits a discrete transition, as illustrated in Fig. 7. However, thermally responsive hydrogels with gentler swelling-temperature response characteristics exist [23], and it may possible to place these hydrogels into the tethered orifices to produce continuous, temperature-based flow control. The response of the MPBA/AAm to changes in either pH or glucose is gradual [14], but we bypassed this aspect by exposing the system to somewhat extreme alternating conditions. Investigation of the present system in a "fluid microcontroller" mode may be of interest, particularly in the thermal case where, as described above, temperature control can be provided by external means.

Despite the increase in speed of response in the present system, the thermal response remains much faster than the response to chemical stimuli. Direct comparisons are somewhat deceiving, since there is no common basis for comparison of the thermal and chemical stimulus magnitude. However, there are basic differences between the mechanisms by which the hydrogel in the microvalve can respond to changes in temperature and chemical environment.

A change in temperature will propagate rapidly through the whole "membrane," including the silicon and hydrogel components. Upon exposure to high temperatures, NIPA hydrogels initially undergo microphase separation, with appearance of water- and polymer-rich microdomains [24]. Even without bulk shrinkage of the hydrogel, this microphase separation may lead to an initial increase in hydraulic permeability [25]. Following this initial step and the accompanying reduction of swelling pressure against the outer orifice wall (see above), the hydrogel will undergo bulk shrinkage and recede from the outer wall, opening up the annular channel for fluid flow. Conversely, a cooling stimulus will be rapidly felt throughout the hydrogel. For both warm and cool stimuli, hydrogel swelling response will be limited primarily by collective diffusion of the crosslinked hydrogel chains in the aqueous solvent [26].

Unlike thermal changes, which are conducted through the whole device, changes in pH or glucose concentration can impact the hydrogel only where the latter is in direct contact with the bathing aqueous medium. When the hydrogel completely fills the orifice (flow suppressed), solutes can only enter at the upstream interface. (Recall that the downstream interface is connected to tubing that is closed off from the external solution.) The solute "invasion" process is thus geometrically constrained in this case, and this may lead to some initial slowing down of response. Once the hydrogel collapses away from the orifice wall, however, solutes may enter by way of the annular gap. Due to the elastic properties of the hydrogel, this gap should originate at the front face and propagate longitudinally. Closure of the valve, however, should occur more uniformly.

More important in determining valve response rate is the relatively slow diffusion of chemical species compared to heat. Furthermore, the hydrogel's response to changes in pH or glucose concentration is due to a change in fixed charge density, which results from the reversible binding of hydrogen ion, hydroxide ion, and glucose to the phenylboronate sidechain of the hydrogel [27]. Slowing of molecular diffusion due to reversible binding is a well-documented phenomenon [28,29], and is the most likely cause of the relatively slow response of the microvalve to chemical changes. In this regard it should be noted that kinetics of response to pH change may be strongly buffer related, since pH buffers act as carriers of acidic protons [30–32], and the same pH change for two different buffer systems may be associated with very different concentrations of acidic protons that are available for transport into and out of the hydrogel. Diffusional transport of other supporting electrolytes, such as NaCl, is relatively rapid in hydrogels [33], and is not expected to limit swelling and deswelling rates in the present system.

As a final comparison, we note that glucose is a larger molecule that hydronium ion, hydroxide ion, and most typical pH buffers. Therefore, its diffusivity will be lower. It is,

therefore, not surprising the response to change in glucose level is not as fast as the pH response. Note, however, that a direct kinetic comparison would require that the changes in fixed charge density on the hydrogel be the same given changes in pH and glucose concentration.

It is noteworthy that hydraulic permeability of the silicon membrane with hydrogel in the collapsed state was much smaller for the pH/glucose-sensitive system than for a temperature-sensitive system. This difference is attributable to the greater degree of collapse exhibited by NIPA hydrogels compared to MPBA/AAm gels.

The leakage observed at high pressure gradients was due to hydrogel failure, not fracture of the tethers. This is not surprising, since hydrogels are notoriously weak materials, weakness being due to inhomogeneities and the tendency to develop high stress fields around fracture seed points. It has recently been demonstrated that the mechanical strength of hydrogels can be greatly increased by co-incorporating a dilute but mobile linear polymer that interpenetrates the primary hydrogel [34]. This second polymer can rapidly move into fracture areas and relieve stress. It is conceivable that with this strategy, the ultimate strength of the tethered construct will depend on the tethers themselves.

6. Conclusions and outlook

We have demonstrated the fabrication of double-sided, tethered structures in silicon membranes. These structures, when loaded with hydrogel, function as a microvalve that can gate fluid flow in response to external stimuli such us temperature, pH, and glucose concentration. The response time for the temperature-sensitive microvalve is of order 10 s, while the pH- and glucose-sensitive microvalves response times are of order 4 min and 10 min, respectively. While these response times are significantly improved compared to previously studied microfabricated systems [14], even faster response times might be achieved by further miniaturization. Another possible improvement would be to provide focused polymerization inside the orifices, perhaps using photoinitiation. This alteration may eliminate the need to peel or scrape off excess hydrogel from the surface, which is both inconvenient and inelegant.

The environmentally sensitive microvalve presented here can be used to implement autonomous systems. For example, it can be integrated within a microreaction chamber having catalysts, enzymes or cells. Reaction or metabolization processes take place in the chamber resulting in a change in certain chemical concentration (e.g. pH or glucose). Once the desired concentration is reached the microvalve orifices open and let the product out. As product is pumped out new reactants or medium enters the chamber. At this point, the chemical concentrations return to the original values and the flow through the microvalve stops, thus initiating a new reaction cycle. Such a system would work without need of additional control electronics.

Acknowledgements

The authors thank the staff of the Nanofabrication Center (NFC) of the University of Minnesota for their assistance. Partial funding for this project was provided by Grant EB003125 from the National Institutes of Health, a grant-in-aid from the Biomedical Engineering Institute at the University of Minnesota, a fellowship from the Spanish Ministry of Education, Culture and Sports for A. Baldi, and a Samuel J. Melendy fellowship to Y. Gu.

Appendix A. Simple model for pressure–flow characteristic

In the microvalve, fluid flow occurs through a channel comprised of an approximately annular gap between the hydrogel surrounding the cylindrical post, and the outer wall of the orifice. Let a, b, and R denote, respectively, the radius of the post, the radius of the orifice, and the distance from the post center to the outer edge of the hydrogel (see Fig. 4a). Let L denote the axial length of the hydrogel. Assuming the usual no-slip boundary condition for fluid flow at the hydrogel surface and the outer wall of the orifice, flow through the channel is given by [35]

$$Q = \frac{\pi b^4 \Delta P}{8\eta L}\left\{1 - \left(\frac{R}{b}\right)^4 + \frac{[1-(R/b)^2]^2}{\ln(R/b)}\right\}$$

where ΔP is the pressure drop across the channel and η is the liquid viscosity.

Assuming that the hydrogel behaves as a linearly deformable medium, and that only axial stress is important in the deformation process, we may write

$$L = L_0\left(\frac{1-\Delta P}{Y'}\right)$$

and

$$R - a = \left(\frac{1+\sigma'\Delta P}{Y'}\right)(R_0 - a)$$

where L_0 and R_0 are the length and outer radius of the hydrogel before deformation, and Y' and σ' represent, respectively, modified Young's modulus and modified Poisson's ratio. Because the shrinking of the hydrogel is constrained by the post, the hydrogel is already in a state of stress, so the values of the elasticity parameters are modified from the values they would take in the free-swelling case.

Fig. 11 depicts a non-dimensionalized pressure–flow characteristic based on this model, with $a = 20\,\mu$m, $b = 70\,\mu$m, and $R_0 = 500\,\mu$m, based on the micrographs in Fig. 4. While we have no direct measurement of the modified Young's modulus and Poisson's ratio, we will, for the present purpose, use data presented by Hirotsu [15] for free deswollen *N*-isopropylacrylamide hydrogels at equilibrium, and estimate that $Y' \sim 30$ kPa and $\sigma' \approx 0.45$. Note that this

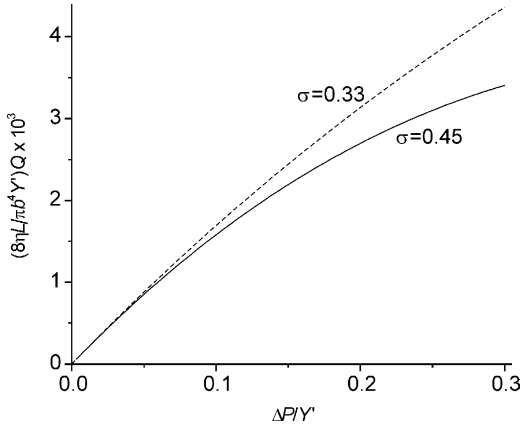

Fig. 11. Predicted dimensionless flow vs. pressure characteristic based on parameters in the Appendix A.

value of Poisson's ratio implies that at equilibrium the hydrogel shrinks upon compression by expelling some of its water. Upon initial compression, water will not have time to leave, and one will have $\sigma' = 0.5$. However, equilibrium is achieved rapidly in the present system due to its small size. The range of $\Delta P/Y'$ shown in Fig. 11 is, therefore, roughly consistent with the range of ΔP explored in Fig. 8. The downward departure from linearity seen in Fig. 8 is qualitatively reproduced in Fig. 11. Because of parameter uncertainties, a direct comparison is not made. However, we also include in Fig. 11 predictions based on $\sigma' = 0.33$. In this case, lateral expansion of the hydrogel does not overcome the effect of axial shortening due to the pressure difference, and the pressure–flow characteristic is nearly linear.

References

[1] T. Tanaka, D. Fillmore, S.-T. Sun, I. Nishio, G. Swislow, A. Shah, Phase transitions in ionic gels, Phys. Rev. Lett. 45 (1980) 1936–1939.
[2] Y. Osada, S.B. Russ-Murphy, Intelligent Gels, Scientific American, May 1993, pp. 82–87.
[3] Q. Luo, S. Mutlu, Y.B. Gianchandani, F. Svec, J.J. Fréchet, Monolithic valves for microfluidic chips based on thermoresponsive polymer gels, Electrophoresis 24 (2003) 3694–3702.
[4] D.J. Beebe, J.S. Moore, J.M. Bauer, Q. Yu, R.H. Liu, C. Devadoss, B.-H. Jo, Functional hydrogel structures for autonomous flow control inside microfluidic channels, Nature 404 (2000) 588–590.
[5] Q. Yu, J.M. Bauer, J.S. Moore, D.J. Beebe, Responsive biomimetic hydrogel valve for microfluidics, Appl. Phys. Lett. 78 (2001) 2589–2591.
[6] A. Richter, S. Howitz, D. Kuckling, K.-F. Arndt, Influence of volume phase transition phenomena on the behavior of hydrogel-based valves, Sens. Actuators B: Chem. 99 (2004) 451–458.
[7] M.E. Harmon, M. Tang, C.W. Frank, A microfluidic actuator based on thermoresponsive hydrogels, Polymer 44 (2003) 4547–4556.
[8] A. Baldi, Y. Gu, P. Loftness, R.A. Siegel, B. Ziaie, A hydrogel-actuated environmentally-sensitive microvalve for active flow control, IEEE J. Microelectromech. Syst. 12 (2003) 613–621.
[9] A.M. Mika, R.F. Childs, J.M. Dickson, Chemical valves based on poly(4-vinylpyridine)-filled microporous membranes, J. Membr. Sci. 153 (1999) 45–56.
[10] Y. Gu, A. Baldi, B. Ziaie, R.A. Siegel, A Micromachined, Hydrogel-Gated Smart Flow Controller, Solid-State Sensor, Actuator, and Microsystems Workshop, Hilton Head, USA, June 2002.
[11] R.A. Siegel, Y. Gu, A. Baldi, B. Ziaie, Novel swelling/shrinking behaviors of glucose-binding hydrogels and their potential use in a microfluidic insulin delivery system, Macromol. Symp. 207 (2004) 249–256.
[12] K.F. Arndt, D. Kuckling, A. Richter, Application of sensitive hydrogels in flow control, Polym. Adv. Technol. 11 (2000) 496–505.
[13] N.C. MacDonald, SCREAM MicroElectroMechanical systems, Microelectron. Eng. 32 (1996) 51–55.
[14] Y. Gu, Swelling Properties of Phenylboronic Acid-containing Hydrogels and their Application in Microfluidic Drug Delivery Devices, Ph.D. Thesis, University of Minnesota, Minneapolis, MN, USA, 2003.
[15] S. Hirotsu, Elastic anomaly near the critical point of volume phase transition in polymer gels, Macromolecules 23 (1990) 903–905.
[16] J. Kost, T.A. Horbett, B.D. Ratner, M. Singh, Glucose-sensitive membranes containing glucose oxidase: swelling, activity, and permeability studies, J. Biomed. Mater. Res. 19 (1985) 1117–1133.
[17] K. Ishihara, M. Kobayashi, N. Ishimaru, I. Shinohara, Glucose induced permeation control of insulin through a complex membrane consisting of immobilized glucose oxidase and a polyamine, Polym. J. 16 (1984) 625–631.
[18] R. Yoshida, K. Sakai, T. Okano, Y. Sakurai, Surface-modulated skin layers of thermal responsive hydrogels as on–off switches. 2. Drug permeation, J. Biomater. Sci. Polym. Ed. 3 (1992) 243–252.
[19] T. Peng, Y.-L. Cheng, Temperature-responsive permeability of porous PNIPAAM-g-PE membranes, J. Appl. Polym. Sci. 70 (1998) 2133–2142.
[20] Z. Hu, C. Wang, K.D. Nelson, R.C. Eberhart, Controlled release from a composite silicone/hydrogel membrane, ASAIO J. 46 (2000) 431–434.
[21] K. Zhang, X.Y. Wu, Modulated insulin permeation across a glucose-sensitive polymeric composite membrane, J. Control. Release 90 (2002) 169–178.
[22] F. Horkay, A.-M. Hecht, E. Geissler, Effect of cross-links on the swelling equation of state: polyacrylamide hydrogels, Macromolecules 22 (1989) 2007–2009.
[23] Y.H. Bae, T. Okano, S.W. Kim, Temperature dependence of swelling of crosslinked poly(*N*-*N*′-alkyl substituted acrylamides) in water, J. Polym. Sci. 28 (1990) 923–936.
[24] Y. Li, G. Wang, Z. Hu, Turbidity study of spinodal decomposition of an *N*-isoproplacrylamide gel, Macromolecules 28 (1995) 4194–4197.
[25] M. Tokita, T. Tanaka, Reversible decrease of gel–solvent friction, Science 253 (1991) 1121–1123.
[26] T. Tanaka, D. Fillmore, Kinetics of swelling of gels, J. Chem. Phys. 70 (1979) 1214–1218.
[27] S.A. Asher, V.L. Alexeev, A.V. Goponenko, A.C. Sharma, I.K. Lednev, C.S. Wilcox, D.N. Finegold, Photonic crystal carbohydrate sensors: low ionic strength sugar sensing, J. Am. Chem. Soc. 125 (2003) 3322–3329.
[28] J.H. Nussbaum, A.J. Grodzinsky, Proton diffusion reaction in a protein polyelectrolyte membrane and the kinetics of electromechanical forces, J. Membr. Sci. 8 (1981) 193–219.
[29] A. English, T. Tanaka, E.R. Edelman, Equilibrium and non-equilibrium phase transitions in copolymer polyelectrolyte hydrogels, J. Chem. Phys. 107 (1997) 1645–1654.
[30] R.A. Siegel, I. Johannes, C.A. Hunt, B.A. Firestone, Buffer effects on swelling kinetics of polyelectrolyte gels, Pharm. Res. 9 (1992) 76–81.
[31] M.J. Lesho, N.J. Sheppard, A method for studying swelling kinetics based on measurement of electrical conductivity, Polym. Gels Netw. 5 (1997) 503–523.
[32] S.K. De, N.R. Aluru, B.B.J. Johnson, W.C. Crone, D.J. Beebe, J. Moore, Equilibrium swelling and kinetics of pH-responsive hydro-

gels: models, experiments, and simulations, J. Microelectromech. Syst. 9 (2002) 544–555.
[33] P.E. Grimshaw, J.H. Nussbaum, M.L. Yarmush, A.J. Grodzinsky, Kinetics of electrically and chemically induced swelling in polyelectrolyte gels, J. Chem. Phys. 93 (1990) 4462–4472.
[34] J.P. Gong, Y. Katsuyama, T. Kurukawa, Y. Osada, Double-network hydrogels with extremely high mechanical strength, Adv. Mater. 15 (2003) 1155–1158.
[35] R.B. Bird, W.E. Stewart, E.N. Lightfoot, Transport Phenomena, Wiley, New York, 1960.

Biographies

Antonio Baldi received his BS degree in telecommunication engineering from the Universitat Politècnica de Catalunya, in 1996. He did research on chemical microsensors at the Centro Nacional de Microelectrónica in Barcelona (CNM-IMB, CSIC) for five years until he received his PhD degree on electronics engineering from the Universitat Autònoma de Barcelona, in 2001. From 2001 to 2003, he was with the UMBM Laboratory at the University of Minnesota, working in the field of bioMEMS as a postdoctoral fellow. His research there was focused on the development of sensors and microfluidic devices incorporating stimuli-sensitive hydrogels. He also was involved in the fabrication and test of inductively coupled wireless MEMS and cell manipulation micro-tools. In the summer of 2003, he joined the Chemical Transducers Group (GTQ), at the Centro Nacional de Microelectrónica, where he works on the development of microsystems and instrumentation for chemical and biochemical sensing.

Ming Lei received his BS degree in chemistry from Nankai University, China, in 1996, first MS degree in polymer physics and chemistry from the Chinese Academy of Sciences, China, in 1999, and second MS degree in materials science and engineering from University of Minnesota, in 2001. He is currently a PhD candidate at the department of electrical engineering, University of Minnesota. His research is focused on hydrogel-based microsystems for chemical sensing and active flow control.

Yuandong Gu received his MEE degree (2001) in electrical engineering and PhD degree in pharmaceutics (2003) at the University of Minnesota. He is currently a research scientist at the Honeywell International Co. His research interests are in the area of biological and chemical sensors.

Ronald A. Siegel is professor and head of the Department of Pharmaceutics, and professor of biomedical engineering at the University of Minnesota. He received his BS degree with honors in mathematics from the University of Oregon, in 1975, and his MS and ScD degrees in electrical engineering and computer science from the Massachusetts Institute of Technology, in 1979 and 1984, respectively. From 1984 to 1998, he was professor of biopharmaceutical sciences and pharmaceutical chemistry at the University of California at San Francisco, and has been at the University of Minnesota, since 1998. His research interests include drug delivery, polymer physical chemistry, microfabrication, membrane transport theory, and application of control theory in the optimization of drug therapy. Dr. Siegel received the Pfizer Young Investigator Grant Award from the American Association of Pharmaceutical Scientists (AAPS) in 1988, and the Young Investigator Award from the Controlled Release Society (CRS) in 1989. He was president of CRS during 1997–1998. In 1999, he was inducted as fellow of the American Institute of Medical and Biological Engineering (AIMBE), and as fellow of AAPS. He presently serves as book review editor of *Journal of Controlled Release*.

Babak Ziaie received his doctoral degree in electrical engineering from the University of Michigan, in 1994. His dissertation was related to the design and development of an implantable single channel microstimulator for functional neuromuscular stimulation. From 1995 to1999, he was a postdoctoral fellow and an assistant research scientist at the Center for Integrated Microsystems (CIMS) of the University of Michigan. He subsequently joined the Electrical and Computer Engineering Department of the University of Minnesota, as an assistant professor (1999–2004). In 2005, he moved to the School of Electrical and Computer Engineering at Purdue University, where he currently is an associate professor. His research interests are mostly related to biomedical applications of MEMS and microsystems. These include implantable wireless microsystems for diagnosis and management of glaucoma, hydrogel-based microsystems for physiological sensing and active flow control, multi-channel wideband wireless interfaces for central nervous system (brain/machine interface), biomimetic structures, and ultra-sensitive sensors for biological (molecular and cellular) applications. Dr. Ziaie is the recipient of the NSF Career Award in Biomedical Engineering (2001) and McKnight Endowment Fund Award for Technological Innovations in Neuroscience (2002). Dr. Ziaie is a member of the IEEE, American Association for the Advancement of Science, and the American Physical Society.